JOURNAL OF APPLIED ELECTROCHEMISTRY 25 (1995) 953–961

Effect of cathodic reduction on catalytic activity of amorphous alloy electrodes for electrooxidation of sulfite

T. MORI*, A. KAWASHIMA, E. AKIYAMA, H. HABAZAKI, K. ASAMI, K. HASHIMOTO

Institute for Materials Research, Tohoku University, Sendai 980-77, Japan

Received 21 November 1994; revised 7 March 1995

Active electrode materials for a new zinc electrowinning process, in which the thermodynamic cell voltage is about half that of the conventional process by replacing oxygen evolution by anodic oxidation of SO_2 produced in the zinc smelting process have been studied. Immersion in HF solution and subsequent cyclic voltammetry (CV) in sulfuric acid are known to be effective surface activation treatments of the amorphous alloy electrodes. The galvanostatic cathodic reduction (CR) treatment was applied to obtain further activation for sulfite oxidation for HF- and CV-treated electrodes prepared from amorphous nickel-valve metal-platinum group metal alloys. This treatment has been found to be effective in enhancing the activity. Among the amorphous Ni–40Nb alloys containing platinum group elements, the platinum-containing electrode showed the highest catalytic activity, which was higher than that of platinized platinum. Furthermore, the electrocatalytic activities of CR-treated electrodes prepared from amorphous alloys containing platinum and rhodium, and platinum and ruthenium were higher than that of the electrode containing only platinum. According to XPS analysis of the amorphous Ni–40Nb–1Pt–1Ru alloy specimen the enrichment of platinum and ruthenium occurred by CV treatment, and a small amount of oxidized platinum and ruthenium species remained on the electrode surfaces, but most of them were cathodically reduced to the metallic state by CR treatment. High catalytic activities for sulfite oxidation can be attributed to the metallic state of platinum and ruthenium contained in the alloy electrodes, even though the activity of these electrocatalysts is higher than that of pure Pt or Ru.

1. Introduction

A substantial part of world zinc production is based on the electrowinning process, since a product of high purity is obtained. For conventional zinc electrowinning, the thermodynamic cell voltage is approximately 2.0 V and oxygen evolved in the cell is an unnecessary byproduct. In addition oxygen gas evolution is responsible for a large part of the practical cell voltage. Insoluble lead–silver alloys have been used as anodes. A new process to reduce the electrical energy consumption involves replacing oxygen evolution by the anodic oxidation of SO_2 [1] produced in the zinc smelting process or by the anodic oxidation of H_2 [2, 3]. In the case of the oxidation of hydrogen, it is necessary to change the electrowinning process and to consider the high cost of the hydrogen gas. When SO_2 dissolves in acid solution, the sulfurous acid (H_2SO_3) is formed and an oxidation reaction of H_2SO_3 occurs on the anode. The thermodynamic cell voltage for zinc winning combined with H_2SO_3 oxidation is about 0.9 V, which is 1.1 V lower than that of the conventional process. To realize the above mentioned new process for the electrowinning of zinc, the anode needs to have high electrocatalytic activity for oxidation of H_2SO_3. Molecular SO_2, and SO_3^{2-} and HSO_3^- ions are present in the aqueous H_2SO_3 solution. A similar environment can be obtained when sodium sulfite is dissolved in aqueous solution. Since sulfite is known to decompose to SO_2 in acidic media and the concentration of SO_2 decreases during nitrogen gas bubbling, a neutral sodium sulfite solution was used.

It was reported previously [4] that ribbon-shaped amorphous nickel-valve metal alloys containing one atomic percent of platinum group elements and other elements showed enhanced activity for anodic sulfite oxidation in a neutral borate buffer solution after activation in HF solution and treatment by cyclic voltammetry (CV) in H_2SO_4 solution. Among them, the amorphous alloys containing platinum showed the highest catalytic activity, which was higher than that of the platinized platinum (pt-Pt) electrode. Furthermore, the combined addition of platinum and ruthenium to amorphous Ni–40(Zr or Nb) alloy led to a very high activity which was higher than those of electrodes prepared from Ni–40(Zr or Nb)–1Pt alloy. However, a quite different anodic oxidation behaviour between Ni–40Zr–1Pt–1Ru and Ni–40Nb–1Pt–1Ru alloy electrodes was observed. Figure 1 shows the polarization curves for HF + CV-treated alloy electrodes measured in 0.075 M $Na_2B_4O_7$ + 0.3 M H_3BO_4 + 1 M Na_2SO_3 at 30 °C. It is clear that the Zr-containing

* Present address: Toho Gas Co., Ltd, 19-18 Sakurada-cho, Atsuta-ku, Nagoya 458, Japan

0021-891X

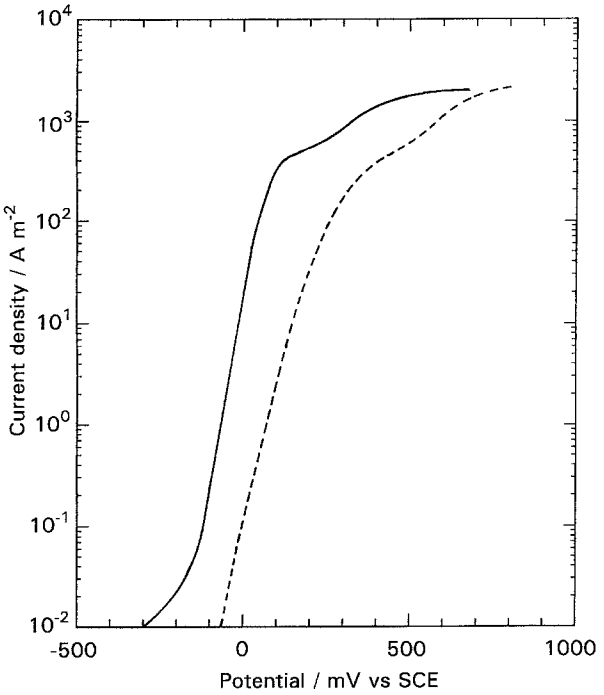

Fig. 1. Potentiodynamic polarization curves of the CV-treated electrodes prepared from the amorphous Ni–40Zr–1Pt–1Ru and Ni–40Nb–1Pt–1Ru alloys for sulfite oxidation measured in a deaerated 0.075 M $Na_2B_4O_7$ + 0.3 M H_3BO_3 + 1 M Na_2SO_3 solution (pH 8.4) at 30 °C and IR free. Key: (——) Zr and (- - - -) Nb.

alloy electrode exhibits a considerably higher catalytic activity for sulfite oxidation than that for the Nb-containing electrode. This suggests that for the Nb-containing alloy electrode, the surface activation by HF + CV treatments is not sufficient to improve the activity.

For further activation of the electrode, a cathodic reduction treatment was applied. The objective of the present work is to evaluate the effect of cathodic reduction on the catalytic activity for anodic oxidation of sulfite on the electrodes prepared from amorphous alloys. XPS measurements have been carried out for these electrodes before and after the cathodic reduction to elucidate the mechanism of the enhanced activity for the sulfite oxidation.

2. Experimental details

Crystalline nickel-valve metal-platinum group metal alloy ingots were prepared by argon arc melting of 99.95% nickel, 99% niobium or zirconium and 99% ruthenium, rhodium, iridium and/or platinum. Amorphous alloys were prepared by a single-roller quenching technique under an argon atmosphere after remelting these alloy ingots. The amorphous alloys were in the form of ribbons of 1–2 mm width and 10–30 μm thickness. The amorphous nature of the alloys was confirmed by X-ray diffraction at θ–2θ mode with CuK_α radiation. The nominal composition of the alloys is given in Table 1.

The surface activation treatment of the alloys was carried out for all the alloys tested by immersion in 0.46–46% HF at room temperature for several minutes to several tens of minutes (HF treatment). With this treatment, a black, porous surface layer about 1 μm thick was formed on the ribbon-shaped electrodes. Cyclic voltammetry (CV) ranging from −200 to 800–1300 mV vs SCE was then carried out with a potential sweep rate of 50 mV s^{-1} in a deaerated 0.5 M H_2SO_4 at 30 °C after HF treatment. The term 'CV-treated' used in the text and figures means that the specimen was treated by HF and CV. For further activation of the CV-treated electrode, a cathodic reduction treatment was performed galvanostatically at 100 μA cm^{-2} for 60 min in deaerated 0.5 M H_2SO_4 at 30 °C.

The electrode characteristics for sulfite oxidation were evaluated by potentiodynamic polarization with a potential sweep rate of 50 mV min^{-1}. Correction for ohmic drop was made using a Hokuto IR Compensation Instrument. Since sulfite is known to decompose to SO_2 in acidic media, the electrolyte used was a deaerated 0.075 M $Na_2B_4O_7$ + 0.3 M H_3BO_3 + 1 M Na_2SO_3 solution (pH 8.4) at 30 °C. The electrochemical surface area was determined using the same method as described previously [5].

X-ray photoelectron spectroscopy (XPS) was applied to five types of specimen including those

Table 1. Nominal composition of amorphous alloys (at %)

Alloy	*Ni*	*Zr*	*Nb*	*Ta*	*Ru*	*Rh*	*Ir*	*Pt*
Ni–40Zr–1Pt	59	40						1
Ni–40Nb–1Ru	59		40		1			
Ni–40Nb–1Rh	59		40			1		
Ni–40Nb–1Ir	59		40				1	
Ni–40Nb–1Pt	59		40					1
Ni–40Nb–2Pt	58		40					2
Ni–40Nb–3Pt	57		40					3
Ni–40Ta–1Pt	59			40				1
Ni–40Zr–1Pt–1Ru	58	40			1			1
Ni–40Nb–0.5Pt–0.5Ru	59		40		0.5			0.5
Ni–40Nb–0.8Pt–0.2Ru	59		40		0.2			0.8
Ni–40Nb–1Pt–1Ru	58		40		1			1
Ni–40Nb–0.5Pt–0.5Rh	59		40			0.5		0.5
Ni–40Nb–0.5Pt–0.5Ir	59		40				0.5	0.5

used for sulfite oxidation at 50 mV vs SCE; (a) as-HF-treated, (b) CV-treated in 0.5 M H_2SO_4, (c) polarized at 50 mV for 30 min in the borate buffer solution containing 1 M Na_2SO_3 after treatment (b), (d) cathodically polarized at 100 $\mu A\,cm^{-2}$ for 30 min in 0.5 M H_2SO_4 after treatment (b) (CR-treated), and (e) polarized at 50 mV for 30 min in the borate buffer solution containing 1 M Na_2SO_3 after treatment (d). After being thus treated, the specimens were rinsed with deaerated distilled water and transferred to the XPS chamber without air exposure. A Shimadzu ESCA 850 electron spectrometer was used to measure X-ray photoelectron spectra excited by the MgK_α line (1253.6 eV). The binding energies of the electrons were determined by a calibration method described elsewhere [6, 7]. A method described by some of the present authors [8, 9] was applied to the quantitative evaluation of the composition of the surface region of the specimen. The composition was calculated without distinguishing the metallic and oxidic states because some of the atoms in metallic states might have been oxidized during the specimen transfer from the solution to the XPS chamber although care was taken to minimize the oxidation as mentioned above. The effect of the contaminant carbon was corrected assuming the carbon layer covers the top of the specimen surface [8, 9]. The photoionization cross section of the Ni $2p_{3/2}$, Nb $3d_{5/2}$, Zr $3d_{3/2}$, Ru $3d_{3/2}$ and Pt $4f_{7/2}$ were 2.32 [9], 2.981 [10], 2.561 [11], 4.449 [11] and 5.01 [12], respectively.

3. Results and discussion

HF-treated amorphous alloys used in this study were passivated spontaneously in the borate buffer solution at pH 8.4 without sodium sulfite and their anodic current densities were less than $4 \times 10^{-1}\,A\,m^{-2}$ up to 800 mV vs SCE. Furthermore, the amorphous alloys without HF-treatment were also passivated spontaneously even in 1.5 M H_2SO_4 at 40 °C and the anodic current densities were less than $10^{-1}\,A\,m^{-2}$ up to 1600 mV vs SCE [13]. Therefore, the amorphous Ni–40Nb alloys possess very high corrosion resistance in acidic and neutral solution.

The electrocatalytic activity for the oxidation of sulfite was greatly improved by applying the cathodic reduction treatment to CV-treated Nb-containing electrodes. The IR-corrected polarization curves for the oxidation of sulfite on the amorphous Ni–40Nb–1Pt–1Ru alloy electrode after the CV treatment and after CR treatment were measured in deaerated 0.075 M $Na_2B_4O_7$ + 0.3 M H_3BO_3 + 1 M Na_2SO_3 solution (pH 8.4) at 30 °C as shown in Fig. 2. It is clear that the cathodically reduced Nb-containing alloy electrode can sustain greater currents at potentials between −50 and 200 mV vs SCE and the polarization behaviour is almost the same as that of the CV-treated Zr-containing alloy electrode shown in Fig. 1. The CR treatment also improved the activity for the Ni–40Zr–1Pt–1Ru alloy electrode, which is not shown in this Figure, although it gave only a slight enhancement.

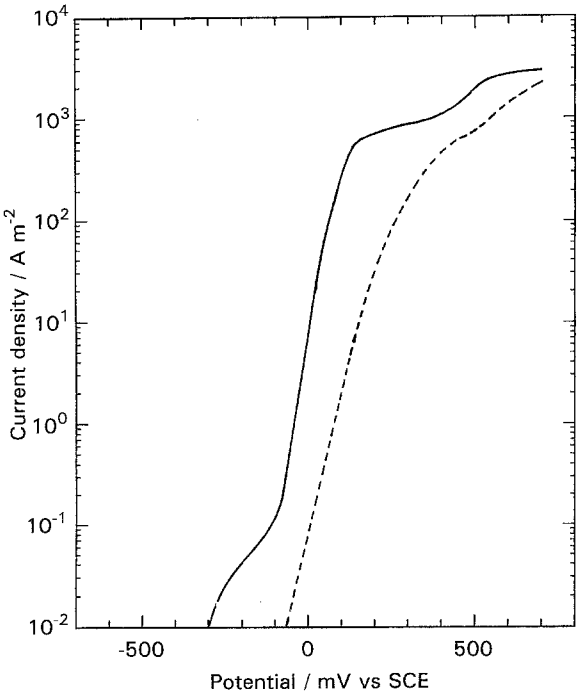

Fig. 2. Potentiodynamic polarization curves of the (- - - -) CV- and (——) CR-treated electrodes prepared from the amorphous Ni–40Nb–1Pt–1Ru alloys for sulfite oxidation measured in a deaerated 0.075 M $Na_2B_4O_7$ + 0.3 M H_3BO_3 + 1 M Na_2SO_3 solution (pH 8.4) at 30 °C and IR free.

Similar results were obtained for Nb-containing electrodes with a single platinum group element. Figure 3 shows the typical performance of CV- and CR-treated amorphous Ni–40Nb–1Pt alloy specimens for sulfite oxidation. The CR treatment for the Ni–40Nb–1Pt alloy specimen also gives remarkable improvement of the catalytic activity. The gradual

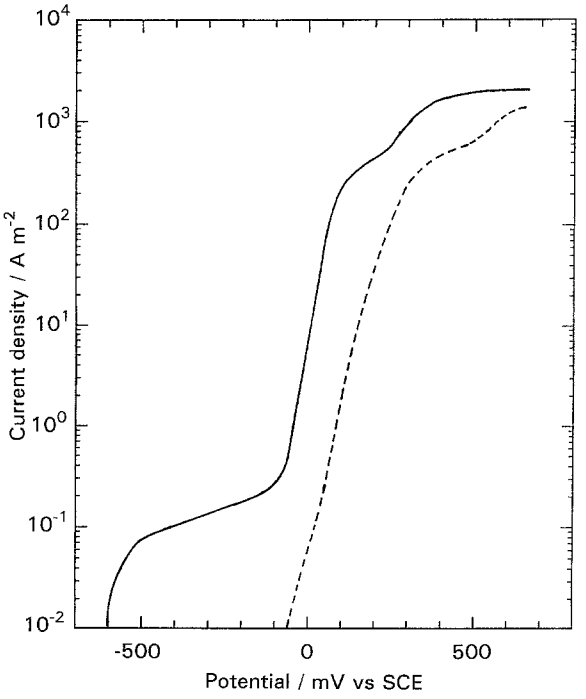

Fig. 3. Potentiodynamic polarization curves of the (- - - -) CV- and (——) CR-treated electrodes prepared from the amorphous Ni–40Nb–1Pt alloys for sulfite oxidation measured in a deaerated 0.075 M $Na_2B_4O_7$ + 0.3 M H_3BO_3 + 1 M Na_2SO_3 solution (pH 8.4) at 30 °C and IR free.

current increase from open circuit potential to about −100 mV vs SCE is probably due to the dissolution of soluble elements remaining on the electrode after various pretreatments, such as HF, CV or CR treatments. This fact has been confirmed by decrease in the current during reverse sweep. The apparent Tafel slope observed from the linear portion of the polarization curve for the CR-treated electrode is about 50 mV (decade)$^{-1}$. Similar results concerning the anodic polarization curves and Tafel slopes were obtained for CR-treated amorphous Ni–40Nb alloy electrodes containing a different single platinum group element and pt-Pt electrode. This suggests that the mechanism of sulfite oxidation on CR-treated electrodes prepared from the amorphous alloys and pt-Pt electrode is not greatly different, although the oxidation mechanism is not clear at the present stage of our work.

Figure 4 summarizes the relation between the activity for sulfite oxidation, expressed in terms of the current density at 50 mV vs SCE, and the alloy platinum-group content. The amorphous alloy electrodes, except for the electrode containing rhodium, have almost the same, or higher, activities for sulfite oxidation than that of the pt-Pt electrode. Among the amorphous Ni–40Nb alloys with a different single platinum group element, the platinum-containing electrode shows the highest catalytic activity, similar to the results for CV-treated electrodes [4]. The value in parentheses in the figure indicates the roughness factor of the electrode. The roughness factor corresponds to the number of catalytically active platinum atoms on the electrode surface, since it is obtained by integrating the hydrogen desorption area in the cyclic voltammogram

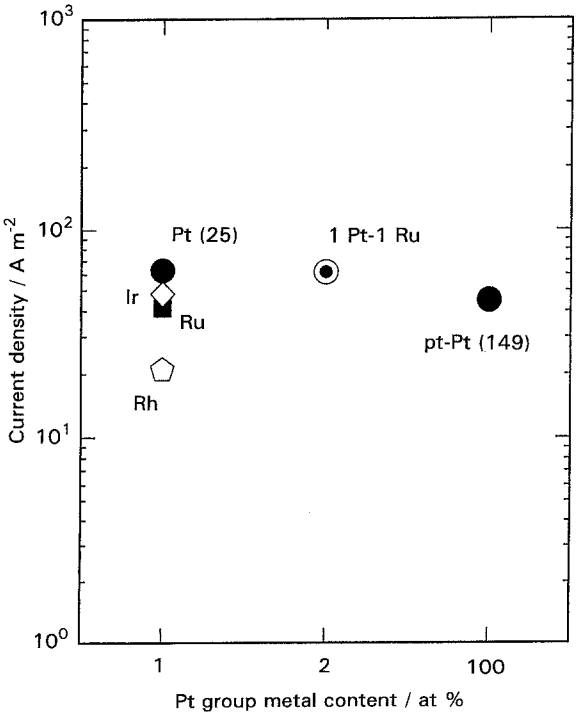

Fig. 4. Current density for the oxidation of sulfite on the CR-treated electrodes prepared from the amorphous Ni–40Nb–x(Ru, Rh, Ir, Pt) alloys polarized at 0.05 V vs SCE, plotted as a function of the alloy platinum group metal content. Measurements were made in the deaerated 0.075 M $Na_2B_4O_7$ + 0.3 M H_3BO_3 + 1 M Na_2SO_3 solution (pH 8.4) at 30 °C.

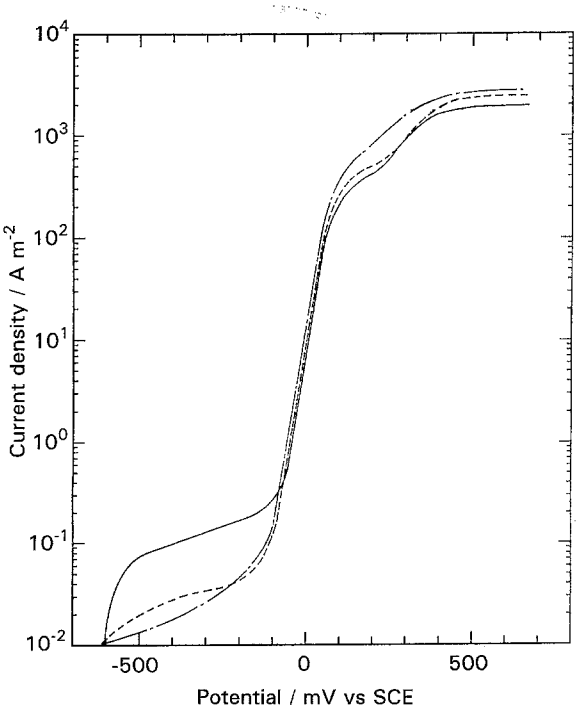

Fig. 5. Potentiodynamic polarization curves of the CR-treated electrodes prepared from the amorphous Ni–40Nb–xPt alloys containing 1–3 at %Pt for sulfite oxidation measured in a deaerated 0.075 M $Na_2B_4O_7$ + 0.3 M H_3BO_3 + 1 M Na_2SO_3 solution (pH 8.4) at 30 °C and IR free. Key: (——) x = 1, (- - - -) x = 2 and (— · — ·) x = 3.

measured in sulfuric acid. Although the pt-Pt electrode has a high roughness factor of 149, the oxidation rate is slightly lower than the platinum containing amorphous alloy electrodes with the roughness factor of 25. This means that the activity of the sulfite oxidation for platinum containing amorphous alloy electrodes is significantly higher than that of the pt-Pt electrode.

The difference in the valve metals, such as Zr, Nb and Ta, in the CR-treated amorphous alloys led to almost no difference in the polarization curves and had no effect on the activity for sulfite oxidation.

To obtain a more active electrode, an attempt was made to increase the alloy platinum content from 1 to 3 at %, since platinum has the highest activity among platinum group metals. Figure 5 compares the polarization curves for CR-treated amorphous Ni–40Nb–xPt alloy electrodes containing 1–3 at % platinum. The activity for the oxidation of sulfite tends to increase with increase in alloy platinum content. The catalytically effective surface area for these alloy electrodes also changes with platinum content.

Figure 6 shows the change in roughness factor (RF) with platinum content. The RF for the CR-treated electrodes increases with increasing platinum content, although it is lower than the corresponding RF of the CV-treated electrodes, possibly due to sintering of nanocrystalline platinum-base alloy particles [14] during CR treatment. This suggests that for Nb-containing amorphous alloys tested in this study the sulfite oxidation activity per number of surface platinum atoms for CR-treated electrodes is essentially higher than that for CV-treated electrodes.

Figure 7 exhibits the change in the anodic current density at 50 mV vs SCE per *RF* as a function of alloy

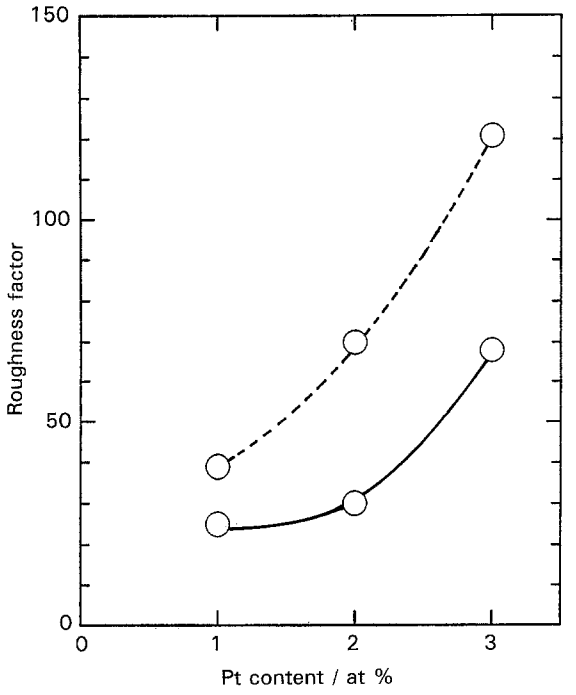

Fig. 6. Change in roughness factor of the electrodes prepared from the amorphous Ni–40Nb–xPt alloys as a function of alloy platinum content measured in 0.5 M H_2SO_4 at 30 °C. Key (- - - -) CV-treated and (——) CR-treated.

platinum content. It is clear that the catalytic activity for sulfite oxidation per number of surface platinum atoms does not change with alloy platinum content up to 3 at%. This indicates that 1 at% platinum addition to amorphous Ni-valve metal alloys is sufficient to confer the catalytic activity.

When two kinds of platinum group elements were contained in the amorphous nickel-valve metal alloy electrodes, the CV-treated electrodes had higher activities for the oxidation of sulfite than those containing

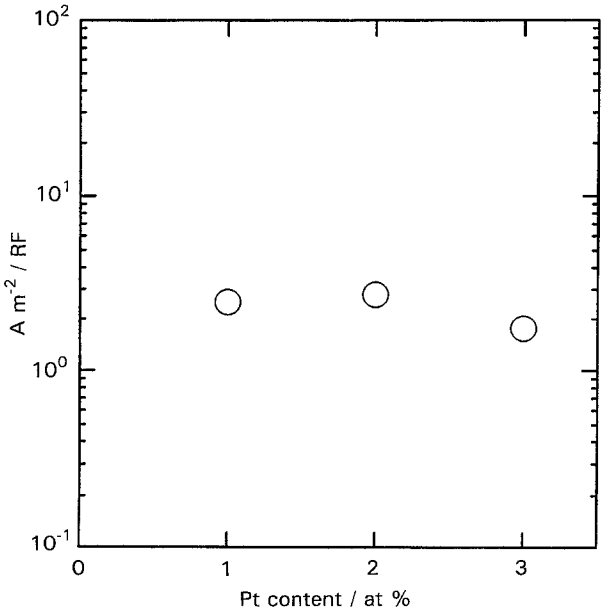

Fig. 7. Change in current density per roughness factor of the electrodes prepared from the amorphous Ni–40Nb–xPt alloys for the oxidation of sulfite as a function of alloy platinum content measured in the deaerated 0.075 M $Na_2B_4O_7$ + 0.3 M H_3BO_3 + 1 M Na_2SO_3 solution (pH 8.4) at 30 °C. CR-treated. E = 0.05 V vs SCE.

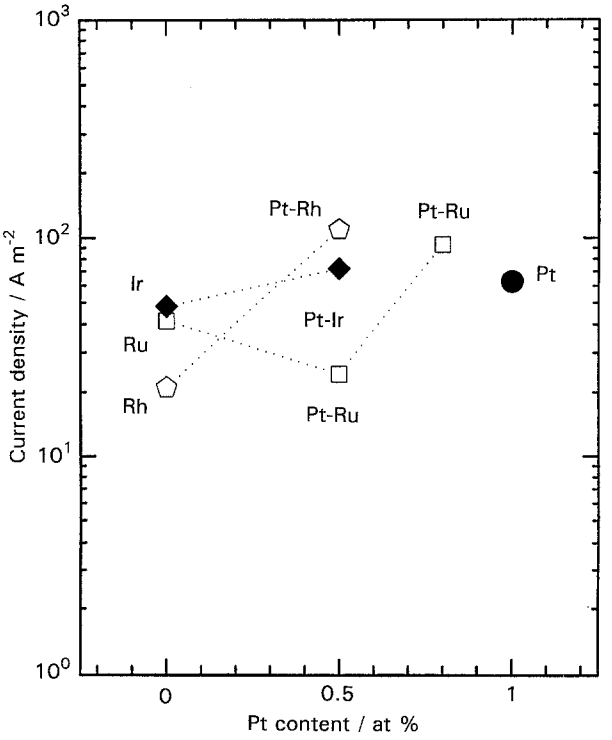

Fig. 8. Current density for the oxidation of sulfite on the CR-treated electrodes prepared from the amorphous Ni–40Nb–xPt–$(1-x)$ (Ru, Rh, Ir) alloys polarized at 0.05 V vs SCE, plotted as a function of the alloy platinum group metal content. Measurements were made in the deaerated 0.075 M $Na_2B_4O_7$ + 0.3 M H_3BO_3 + 1 M Na_2SO_3 solution (pH 8.4) at 30 °C. E = 0.05 V vs SCE.

a single platinum group element [4]. Therefore, the CR treatment was applied to the electrodes prepared from the amorphous alloys containing two kinds of platinum group elements and the catalytic activities were examined. Figure 8 summarizes the change in the current density of sulfite oxidation as a function of alloy platinum content for the amorphous Ni–40Nb alloy electrodes containing different sets of two kinds of platinum group elements. Included in this Figure, for comparison, are the current densities for Ni–40Nb alloy electrodes containing a single platinum group element. It is noted that the electrodes prepared from the amorphous Ni–40Nb–0.5Pt–0.5Rh, Ni–40Nb–0.5Pt–0.5Ir and Ni–40Nb–0.8Pt–0.2Ru alloy electrodes have higher activities than those of the electrode prepared from the Ni–40Nb–1Pt alloy electrode, and pt-Pt electrode (refer to Fig. 4). It can, therefore, be said that rhodium, iridium or ruthenium is an effective promotor of sulfite oxidation.

For a better understanding of such an enhanced activity by the addition of ruthenium, XPS analysis was applied to the amorphous Ni–40(Zr, Nb)–1Pt–1Ru alloys. In general, the kinetics of the reaction depends on surface phenomena. The results of XPS spectra do not necessarily represent the state of the metal surface in the solution during the reaction; that is, the surface in the solution is not exactly the same as that after removal from the solution and transfer into vacuo. At the same time, it is well known that there are many cases where the results of the *ex situ* surface analysis give good clues for the kinetics of the reaction [12]. The spectra over the wide binding

energy region showed peaks of oxygen, sulfur and carbon in addition to those of alloy constituents. The XPS spectrum of boron arising from the solution species was weaker than the detection level. Judging from the peak position of the C 1*s* spectrum, it comes from so-called contaminant carbon, which mainly consists of hydrocarbons. Its origin cannot be specified clearly. In the present case, it might be contaminated during specimen handling, since the XPS intensity of the contaminant carbon changed from specimen to specimen. Carbon contamination cannot easily be avoided even by very careful specimen handling. The S 2*p* spectrum, which was observed in CV- or CR-treated or polarized specimens, showed two or three peaks with binding energies of ~ 162, and 169 eV for CV- or CR-treated specimens, and ~ 167 and 169 eV for the polarized specimens. The peaks at about 162, 167 and 169 eV correspond to S^{2-} [15–17], SO_3^{2-} [16, 18] and SO_4^{2-} [16, 17] states, respectively. The Ni $2p_{3/2}$ spectrum consisted of two peaks of Ni^{2+} and metallic state (Ni^m) whose binding energies were about 865 and 853 eV, respectively. The oxidized nickel species in the surface film formed on these amorphous alloys was mostly removed by CV treatment. The peak at about 207 eV was assigned to Nb^{5+} $3d_{5/2}$ electrons. Nb^m gave a Nb $3d_{5/2}$ peak at ~ 203 eV. The Zr $3d_{5/2}$ spectrum in the air-formed film was composed of two peaks; a Zr^{4+} state peak at 182.4 eV and a Zr^m state peak at 178.7 eV. After CV and CR treatment, no metallic Zr was detected, but Nb oxide was reduced slightly after CR treatment, since Zr oxide is thermodynamically more stable than Nb oxide. The standard free energies of formation for ZrO_2 and Nb_2O_5 are -245.28 and -137.46 kcal at 30 °C, respectively [19].

The platinum 4*f* spectrum consisted of a doublet appearing at 71.6 and 74.9 eV, which was assigned to the metallic state, Pt^m, although the binding energies of Pt $4f_{7/2}$ electrons is higher than that for pure platinum metal (71.2–71.4 eV [12, 20–22]). This difference in the Pt^m $4f_{7/2}$ spectrum can be interpreted in terms of alloying effects. Figure 9 compares the platinum 4f spectra obtained from the surfaces of (a) the amorphous Ni–40Zr–1Pt–1Ru and (b) Ni–40Nb–1Pt–1Ru alloy specimens with various treatments; CV treatment, CV treatment followed by anodic polarization at 50 mV vs SCE for 30 min (designated 'CV + 50 mV'), CR treatment and CR treatment followed by anodic polarization at 50 mV vs SCE for 30 min ('CR + 50 mV'). Included in this figure is the Pt^m 4*f* spectrum shown by a dotted curve, which is obtained from the argon ion etched amorphous Ni–40Nb–1Pt–1Ru alloy for comparison. It is apparent that the Pt spectra obtained from the Ni–40Zr–1Pt–1Ru alloy specimen consist mostly of metallic state peaks and are not greatly changed by CR treatment. This indicates that reduction of platinum for the Zr-containing alloy has been substantially achieved in the process of CV treatment. On the other hand, the Pt 4*f* spectra for Ni–40Nb–1Pt–1Ru is changed by CR treatment. The change is shown in detail in Fig. 10. It can be seen that the CR treatment effectively

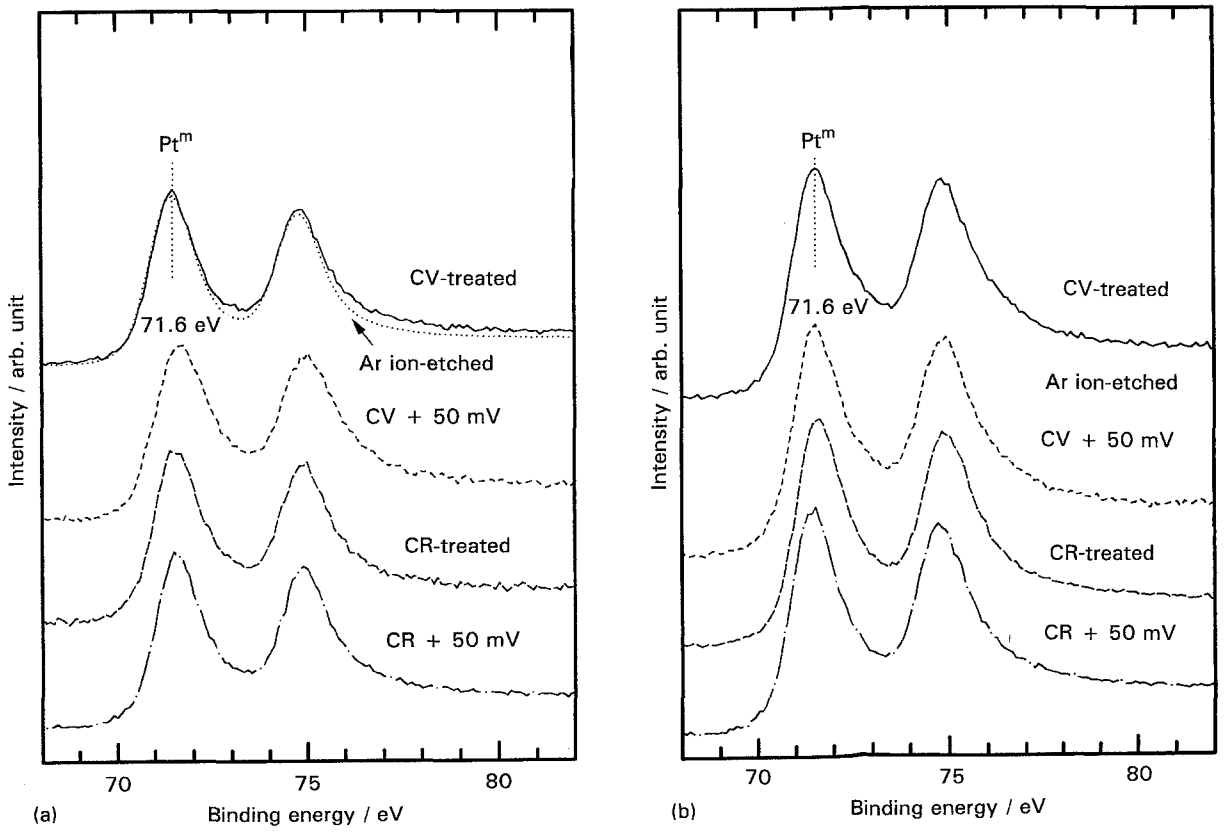

Fig. 9. Pt $4f_{7/2,5/2}$ photoelectron spectra obtained from (a) the amorphous Ni–40Zr–1Pt–1Ru alloy and (b) Ni–40Nb–1Pt–1Ru alloy specimens after various treatments.

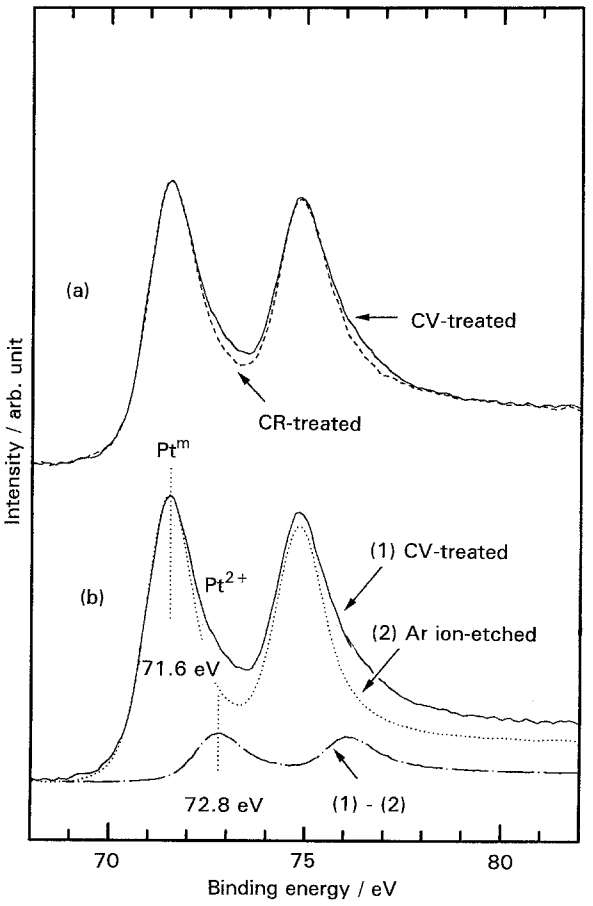

Fig. 10. Pt $4f_{7/2,5/2}$ photoelectron spectra obtained from the CV- and CR-treated amorphous Ni–40Nb–1Pt–1Ru alloy specimens; (a) overlaying the spectra of CV-treated specimen with that of CR-treated specimen, (b) separation of Pt^m and Pt^{2+} spectra from the Pt $4f$ spectrum measured from the CV-treated amorphous alloy specimens.

reduces the oxidized species of platinum remaining on the CV-treated specimen surface, as shown in Fig. 10(a). Figure 10(b) shows the Pt $4f$ spectrum of CV-treated specimen and the Pt^m $4f$ spectrum obtained after argon ion etching of the specimen, together with their differential spectra. The differential spectrum shows a Pt $4f_{7/2}$ peak at 72.8 eV, which is assigned to the Pt^{2+} state since this value is situated between 72.2 eV [12] and 73.4 eV [20] obtained from PtO. A very small amount of Pt^{2+} ions remained, although Pt^{2+} ions were mostly reduced by CR treatment, probably due to insufficient deaeration of the solution and distilled water for rinsing the specimen.

Figure 11 shows Ru $3d_{5/2,3/2}$ spectra obtained from both the amorphous Ni–40Zr–1Pt–1Ru and Ni–40Nb–1Pt–1Ru alloy specimens with various treatments. A dotted curve in this figure is a Ru^m $3d$ spectrum obtained from the argon ion-etched amorphous Ni–40Nb–1Pt–1Ru alloy for comparison. Since the Ru $3d_{3/2}$ peak is overlapped with the contaminant C $1s$ peak, the integrated intensity of the C $1s$ area was estimated from the Ru $3d_{5/2}$ peak intensity assuming the integrated intensity ratio of $Ru_{3/2}$ peak to the Ru $3d_{5/2}$ peak is constant. Ru $3p$ signals were too weak to be analysed. However, the Ru $3d$ signals could offer some information about the presence of metallic or oxidized ruthenium. For the Ni–40Zr–1Pt–1Ru alloy specimen, the peaks at 280.0 eV and 284.1 eV correspond to the metallic Ru $3d_{5/2}$ and $3d_{3/2}$, respectively [23, 24]. The Ru $3d$ spectra for this alloy specimen, before and after CR treatment, exhibit virtually no change. In contrast, for the

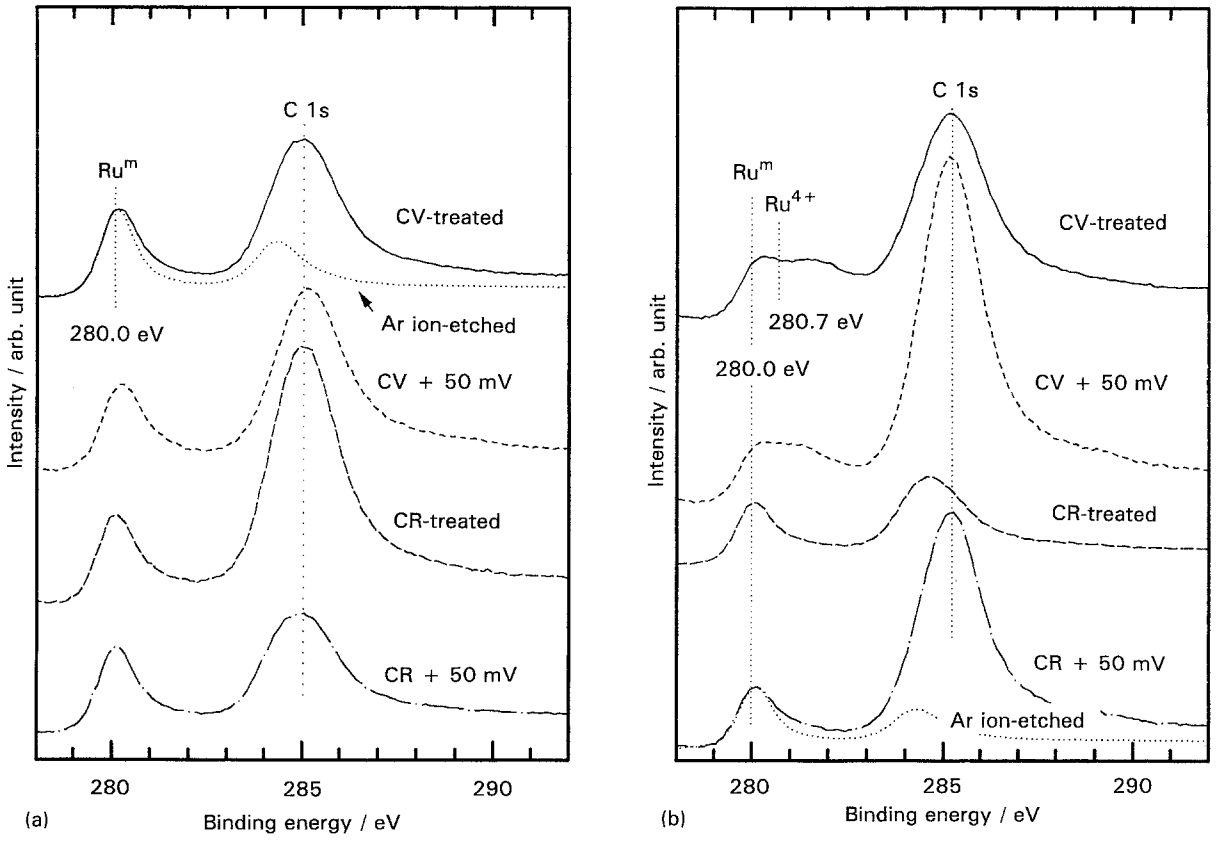

Fig. 11. Ru $3d_{5/2,3/2}$ photoelectron spectra obtained from (a) the amorphous Ni–40Zr–1Pt–1Ru and (b) Ni–40Nb–1Pt–1Ru alloys during a course of a sequence of the treatments.

Ni–40Nb–1Pt–1Ru alloy, the Ru 3*d* spectrum is considerably changed by CR treatment. Before CR treatment, the major ruthenium species is Ru^m, but there are broad peaks between 280eV and 282eV. This might be due to the presence of a certain amount of oxidized ruthenium species such as RuO_2 or RuO_3, since the binding energies for Ru^{4+} and Ru^{6+} $3d_{5/2}$ electrons are reported as 280.7 and 282.4 eV, respectively [23, 24]. After CR treatment, virtually no signals from the oxidized ruthenium are observed. Therefore, from the photoelectron spectra for the amorphous Ni–40Nb–1Pt–1Ru alloy electrode, it can be seen that the oxidized platinum and ruthenium on the surface after CV treatment are substantially reduced to the metallic state of these elements by CR treatment. It can be said that these metallic species have high catalytic activities for the oxidation of sulfite. For the amorphous Ni–40Zr–1Pt–1Ru alloy electrode, platinum and ruthenium are mostly in the metallic state, even after CV treatment, resulting in high catalytic activity. Hence, after CR treatment the electrode prepared from the amorphous Ni–40Zr–1Pt–1Ru and Ni–40Nb–1Pt–1Ru alloys show virtually no difference in activity.

The fact of relatively larger amounts of oxidized species of Pt and Ru for the Nb-containing alloy specimen compared with the Zr-containing alloy specimen in the surface layer may be attributed to different drying process after HF immersion. Even if small amounts of platinum group metals are added to amorphous Ni–40Zr and Ni–40Nb alloys, their catalytic activity for sulfite oxidation is too low for use as an anode for electrowinning of zinc and must be increased by surface activation treatment. Immersion in 46% HF solution and subsequent CV in sulfuric acid are known to be effective surface activation treatments of the electrodes prepared from the amorphous alloys [5, 14, 25–30]. In this experiment, for the Nb-containing alloy, HF treatment was performed by immersion in 46% HF solution for several minutes, followed by drying in air. On the other hand, for the Zr-containing alloy, HF treatment was performed by immersion in dilute HF (0.46%) solution for a relatively long period of time (several tens of minutes). After HF treatment the specimen was immersed in distilled water for several tens of minutes so as not to contact air, because the reactivity of the alloy is very high and the alloy specimen is burned by direct air exposure. Consequently, the extent of air oxidation for the Nb-containing alloy is more severe than that for the Zr-containing alloy; hence relatively large amounts of oxidized Pt and Ru species were formed on the Nb-containing alloy specimen.

The composition of the electrode surface film may be related to the catalytic properties. As mentioned in Section 2, each composition shown in Fig. 12 is the sum of the metallic and oxidic states, and is expressed as a fraction among the metallic elements. Figure 12 shows the change in surface composition for the amorphous Ni–40Zr–1Pt–1Ru and Ni–40Nb–1Pt–1Ru alloys during a course of a series of sequential treatments. The abscissa corresponds to the sequence of the treatments. For the amorphous Ni–40Zr–1Pt–1Ru alloy electrode, HF immersion results in nickel enrichment as a result of the preferential dissolution of zirconium. CV treatment in sulfuric acid leads to considerable enrichment of platinum and ruthenium in the alloy surface. The ratio of platinum to ruthenium is about 1 : 1. The platinum content and the ratio of platinum to ruthenium, which may affect the activity, does not change before and after CR treatment. On the other hand, for the amorphous Ni–40Nb–1Pt–1Ru alloy electrode, the platinum content increases as a result of the decrease in ruthenium and niobium contents by CR treatment. This suggests that niobium transfers from the surface layer to the solution during cathodic reduction, since niobium in the form of oxide can not be removed by CR treatment. At the same time some ruthenium also seems to transfer with the niobium. In this manner, the catalytically active platinum content increases during CR treatment, resulting in high catalytic activity for sulfite oxidation.

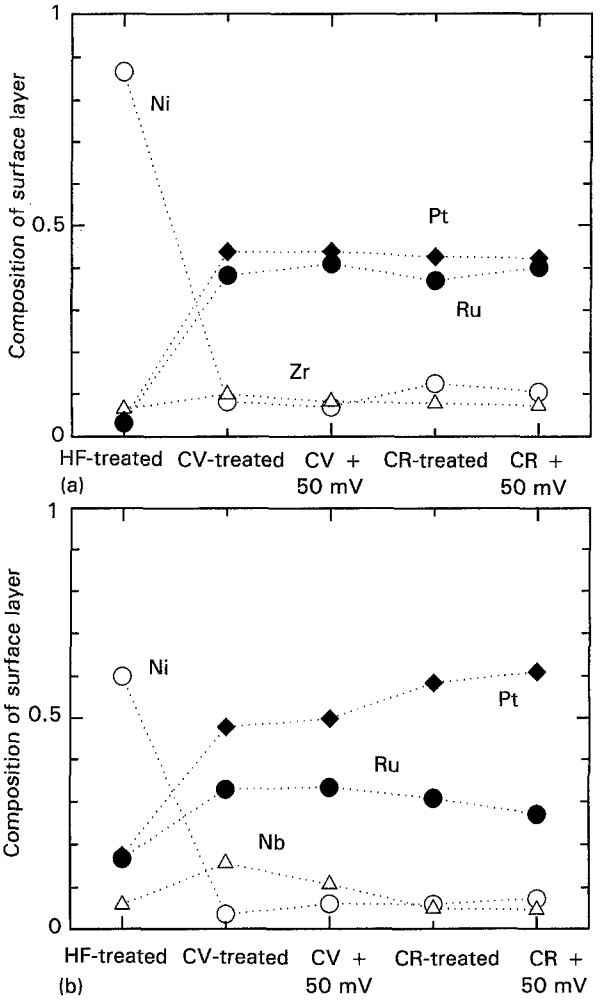

Fig. 12. Change in the surface composition of the electrodes prepared from the amorphous (a) Ni–40Zr–1Pt–1Ru and (b) Ni–40Nb–1Pt–1Ru alloys during a course of a sequence of the treatments. The abscissa corresponds to the sequence of the treatments.

Thus, the enrichment of catalytically active platinum group metals in the surface layer of the electrodes and those in the metallic state are responsible for the high catalytic activity for sulfite oxidation.

4. Conclusions

The following conclusions can be drawn from the investigation of the effect of cathodic reduction on the catalytic activity of sulfite oxidation for the amorphous Ni–40 at % valve-metal alloys containing different platinum group elements:

(i) Galvanostatic cathodic reduction after CV treatment has been found to be effective for further activation of the electrodes prepared from the amorphous alloys.

(ii) Among platinum group elements contained in the CR-treated amorphous alloy electrodes, the increasing order of sulfite oxidation activity is rhodium < ruthenium < iridium < platinum. The activity of these alloy electrodes except the electrode containing rhodium for sulfite oxidation is the same or higher than that of the platinized platinum electrode. The difference in the valve metal, such as Zr, Nb or Ta, has almost no effect on the activity.

(iii) The activity tends to increase with increasing alloy platinum content in amorphous Ni–40Nb–(1–3)Pt alloy electrodes, but there is virtually no change in the activity per number of surface platinum atoms.

(iv) Combined additions of platinum and other platinum group elements to amorphous Ni–40Nb alloy improve the catalytic activity. In particular, substitution of ruthenium, rhodium or iridium for a part of the platinum is very effective.

(v) The enrichment of platinum and ruthenium occurs by CV treatment and oxidized species of platinum and ruthenium on the electrode prepared from the Ni–40Nb–1Pt–1Ru is mostly reduced to the metallic state by the CR treatment. Platinum and ruthenium in the metallic state are found to contribute to the catalytic activities for sulfite oxidation for the electrodes derived from amorphous Ni-valve metal alloys.

Acknowledgements

The authors thank Takeo Nihei of the Institute for Materials Research, Tohoku University for preparing the glass cells. The present work is supported in part by a grant-in-aid for Scientific Research (A) 03403012 and (A) 06402051 from the Ministry of Education, Science and Culture, Japan.

References

[1] N. Furuya and N. Mineo, *Denki Kagaku* **56** (1988) 660.
[2] N. Furuya and S. Motoo, *J. Electroanal. Chem.* **179** (1984) 297.
[3] V. Nikolova, I. Nikolov, T. Vitanov, A. Mobius, W. Schneider and K. Wiesenner, *J. Appl. Electrochem.* **17** (1987) 322.
[4] T. Mori, E. Akiyama, H. Habazaki, A. Kawashima, K. Asami and K. Hashimoto, *Mater. Sci. Engng.* **A181/A182** (1994) 1081.
[5] A. Kawashima, T. Kanda and K. Hashimoto, *ibid.* **99** (1988) 521.
[6] K. Asami, *J. Electron Spectrosc.* **9** (1976) 469.
[7] K. Asami and K. Hashimoto, *Corros. Sci.* **17** (1977) 559.
[8] K. Asami, K. Hashimoto and S. Shimodaira, *ibid.* **17** (1977) 715.
[9] K. Asami and K. Hashimoto, *ibid.* **24** (1984) 83.
[10] E. Hirota, H. Yoshioka, H. Habazaki, A. Kawashima, K. Asami and K. Hashimoto, *ibid.* **32** (1991) 1213.
[11] J. H. Scofield, *J. Electron Spectrosc.* **8** (1976) 129.
[12] M. Hara, K. Asami, K. Hashimoto and T. Masumoto, *Electrochim, Acta* **28** (1983) 1073.
[13] N. Kumagai, Y. Samata, A. Kawashima, K. Asami and K. Hashimoto, *in* 'Corrosion electrochemistry and catalysis of metallic glasses', (edited by R. B. Diegle and K. Hashimoto), The Electrochemical Society, Pennington, NJ (1988) p. 390.
[14] A. Kawashima, T. Kanda, K. Asami and K. Hashimoto, *in* 'Corrosion electrochemistry and catalysis of metallic glasses', (edited by R. B. Diegle and K. Hashimoto), The Electrochemical Society, Pennington, NJ (1988) p. 401.
[15] T. A. Patterson, J. C. Carver, D. E. Leyden and D. M. Hercules, *J. Phys. Chem.* **80** (1976) 1702.
[16] R. J. Bird and G. D. Galvin, *Wear* **39** (1976) 143.
[17] K. Asami and K. Hashimoto, *Trans JIM.* **20** (1979) 119.
[18] B. J. Lindberg, K. Hamrin, G. Johansson, U. Gelius, A. Fahlmann, C. Nordling and K. Siegbahn, *Phy. Scr.* **1** (1970) 277.
[19] O. Kubaschewski and C. B. Alcock, 'Metallurgical thermochemistry', Pergamon Press, Oxford (1979).
[20] J. B. Goodenough, A. Hamnett, B. J. Kennedy, R. Manoharan and S. A. Weeks, *J. Electroanal. Chem.* **240** (1988) 133.
[21] A. Hamnett, B. J. Kennedy and F. E. Wagner, *J. Catal.* **124** (1990) 30.
[22] A. Hamnett and B. J. Kennedy, *Electrochim. Acta* **33** (1988) 1613.
[23] R. Kotz, H. J. Lewerenz and S. Stucki, *J. Electrochem. Soc.* **130** (1983) 825.
[24] K. S. Kim and N. Wignograd, *J. Catal.* **35** (1974) 66.
[25] N. Kumagai, Y. Samata, A. Kawashima, K. Asami and K. Hashimoto, *J. Appl. Electrochem.* **17** (1987) 347.
[26] A. Kawashima, K. Asami and K. Hashimoto, *Mater. Sci. Engng.*, **A134** (1991) 1070.
[27] Y. Hayakawa, A. Kawashima, K. Asami and K. Hashimoto, *J. Appl. Electrochem.* **21** (1992) 1017.
[28] T. Shimada, A. Kawashima, H. Habazaki, K. Asami and K. Hashimoto, *Sci. Rep. Res. Inst. Tohoku Univ.* **A38** (1993) 63.
[29] A. Kawashima, K. Takamura, T. Shimada, H. Habazaki, K. Asami and K. Hashimoto, 'Corrosion, electrochemistry and catalysis of metastable metals and intermetallics' (edited by C. R. Clayton and K. Hashimoto), The Electrochemical Society, Pennington, NJ (1994) p. 346.
[30] K. Takamura, H. Habazaki, K. Kawashima, K. Asami and K. Hashimoto, *Mater. Sci. Engng* **A181/A182** (1994) 1137.